

Characterization of the Confidentiality of a Green Time Reversal Communication System: Experimental Measurement of the Spy BER Sink

D.-T. Phan-Huy*, T. Sarrebourse*, A. Gati*, J. Wiart*

*Orange Labs
92794 Issy-Les-Moulineaux, France

M. H  lard**

** INSA, IETR, UEB
35708 Rennes, France

Abstract—Time Reversal (TR) is a multiple-input single-output (MISO) pre-filtering technique that allows a signal to be sent towards a target antenna by focusing the wave at the receiver both in the time and in the space domains. Recently, TR has been advertised for both green communications and confidential communications. This paper proposes an experimental characterization of the confidentiality of an indoor MISO-TR communication. The transmit system is made of 16 transmit antennas distributed within a room and the data stream is transmitted with a 256-Quadratic Amplitude Modulation (256QAM). The received signal is demodulated by the target user but also by a spy or eavesdropper antenna, both using a Single Tap Receiver. The Bit Error Rate (BER) achieved by the spy is then evaluated for variable positions of the spy nearby the target. The “spy BER” is plotted as a function of the spy-to-target distance. This experimental measurement clearly shows the presence of a spy BER “sink” centered on the target.

Keywords-component: green, Time Reversal, confidentiality, MISO, spy, secure, experimental.

I. INTRODUCTION

In wireless Multiple Input Single Output communication (MISO) systems, high spectral efficiency can be achieved by using channel knowledge at the transmitter to pre-filter the signal. Among low complexity pre-coding schemes, Time Reversal (TR) merely consists in using the time reverse of the channel impulse response as a pre-filter [1]. As firstly demonstrated for underwater acoustics experiments, TR enables to focus the transmit wave both in time and space domains. Moreover, the richer the scattering propagation channel, the higher the focusing gains [2]. Therefore, TR was also proposed for UWB and WLAN systems especially for Time Division Duplex (TDD) transmissions where channel reciprocity can be easily used [3] as well as a larger the number of transmit antennas to achieve high interference alleviation and large multi-path diversity gain [3-5]. Moreover, since TR uses the channel impulse response of the reverse channel as the matched filter, TR provides optimal Bit Error Rate (BER) performance at low Signal To Noise (SNR) ratios when interference becomes much lower than noise, and that even with a simple “single tap” receiver [3].

Very recently, [5] has shown by simulations and experimental measurements that TR is an excellent candidate

for green communications. In fact, owing to the focusing gain, TR enables power consumption to be reduced compared to classical schemes achieving the same performance. The good expected confidentiality property of TR, first mentioned in [5], makes TR a good candidate for secret communications owing to its spatial focusing property combined with its temporal focusing property. Finally, [6] shows that the development of small cells in urban areas, the high densification of access points and transmit antennas, can bring energy savings. In this context, there is a potential for green time reversal communication, in indoor, with a large number of distributed antennas.

Many very complete experimental studies on time reversal (especially on UWB) [7-14] have been held to assess the performance of TR at the target receive antenna: from Signal to Noise and Interference Ratio (SINR) computations up to real over-the-air data transmission using FPGA platforms [12]. However, up to now, no study has assessed the confidentiality of TR. By confidentiality, we mean that signal can be successfully demodulated only at the target antenna, and not around the target antenna by a spy or a eavesdropper antenna.

In this paper, we propose to characterize the confidentiality of a TR indoor communication, between a network of several distributed antennas and one target antenna. We introduce a new metric: the BER achieved by a spy antenna nearby the target one. Section II defines the Spy BER metric. Section III, describes our experimental method to measure the spy BER. Section IV, analyses our spy BER experimental measurements. Section V concludes this paper.

Notation: $i, k, k_1, k_{\text{synchro}}, n, p, t, C, M, N, P, d_i, N_1, N_2, N_{\text{bits}}, N_u \in \mathbb{N}$.

S_{time} is a time interval, S_O and S_G are set indices.

$B, F_C, F_O, F_G, BER^p, p_n^p, q_n^p, r_k, s_k, x_k^{0,i}, y_k^{0,i}, w_k^{0,i}, Y_k^{p,i}, \xi_k^p, W_k^{p,i} \in \mathbb{R}$.

$a_n, \hat{a}_n^p, b_n, \hat{b}_n^p, d_i, \hat{d}_i, \hat{d}_i^p, \epsilon_n^a, \epsilon_n^b, \Gamma, \gamma_k^p, \vartheta_k^p, \theta^p, \Theta^p, \lambda_k^p, \omega_k^p, \zeta^p$ and $\tau \in \mathbb{R}$.

The following are real functions of time t : $f, y, \varphi, \text{co}, \text{si}, u, m^i, \psi^i, h^{p,i}, v^{0,i}, U^{0,i}, V^{p,i}$. $y(t) = 1$ if $0 \leq t < 1$, $t = 0$ otherwise in order to simplify some equation writings, we define: $\text{si}(t) = \sin(2\pi F_c t)$ and $\text{co}(t) = \cos(2\pi F_c t)$

II. THE SPY BER METRIC

This section proposes a characterization method and a spy BER metric to assess the confidentiality of a Time Reversal communication, as illustrated in Fig. 1.

The considered MISO TR system is made of M distributed transmit antennas (numbered with index $i = 0 \dots M - 1$) distributed within in a room and a receiver with 1 target receive antenna as represented in Fig.2. The aim of the MISO TR is to focus the transmit data wave towards the target receive antenna that is set at position number $p = 0$. The Bit Error Rate BER^0 achieved at the receiver with the target antenna is assessed. The aim of the experiment consists in evaluating the Bit Error Rate BER^p of any spy antenna that would be positioned nearby the target antenna at different positions, numbered with index $p = 1 \dots P - 1$. We propose to evaluate BER^p versus p representing a spatial parameter, to characterize the confidentiality of the data transmission. The larger BER^p for positions $p > 0$ far from the target position $p = 0$, the more confidential the communication.

The following paragraphs further define mathematically the BER^p metric.

Let $h^{p,i}(t)$ be the channel impulse response (in the system of bandwidth equal to B centered around the carrier frequency F_C) between transmit antenna i and the spy antenna at position p . $h^{p,i}(t)$ includes antenna gains, path loss, shadowing and fast fading.

The transmitter sends N_{bits} data bits d_j ($j = 0 \dots N_{bits} - 1$) using a Quadratic Amplitude Modulation (QAM) with constellation of size C . The number of symbols to transmit is $N_u = N_{bits} / \log_2(C)$. For each symbol $a_n + jb_n$ of index $n = 0 \dots N_u - 1$, the coefficients a_n and b_n are sent over the cosine and sine parts of the carrier, respectively. a_n and b_n are associated to bits $d_{\log_2(C)n+k}$ with $k = 0 \dots \log_2(C) - 1$. Assuming a transmission in bandwidth equal to B , after a filtering with $f(t)$, square raised root cosine filter with roll-off factor β , the data signal to be transmitted can be expressed as:

$$\varphi(t) = \sum_{n=0}^{N_u} (a_n \cos(t) + b_n \sin(t)) f\left(t - \frac{n}{B}\right). \quad (1)$$

Owing to channel reciprocity, for each antenna m , TR pre-filtering can be applied with $w^i(t) = h^{0,i}(-t)$. Therefore, the signal $\psi^i(t)$ transmitted by antenna i , and normalized to ensure a peak power equal to Γ is given by:

$$\psi^i(t) = \sqrt{\Gamma} \frac{(\varphi * w^{0,i})(t)}{\max_{\tau} \left(\left| \sum_{i=0}^{M-1} (\varphi * w^{0,i})(\tau) \right| \right)}. \quad (2)$$

The signal received at the position p , and coming from all transmit antennas after propagation through $h^{p,i}$ is given by:

$$\theta^p(t) = \sqrt{\Gamma} \sum_{i=0}^{M-1} (\psi^i * h^{p,i})(t). \quad (3)$$

Assuming a single tap receiver and perfect synchronization, perfect peak amplitude estimation of $\theta^p = \max_{\tau} (|\theta^p(t)|)$, with noise ε_n^a and ε_n^b over the cosine and sine parts, the output of the single tap receiver is given by:

$$\hat{a}_n^p = \frac{1}{\theta^p} (\theta^p * \cos * f) \left(\frac{n}{B} \right) + \varepsilon_n^a. \quad (4)$$

$$\hat{b}_n^p = \frac{1}{\theta^p} (\theta^p * \sin * f) \left(\frac{n}{B} \right) + \varepsilon_n^b. \quad (5)$$

The de-mapping is then performed to estimate the bits $\hat{d}_{\log_2(C)n+k}$ based on \hat{a}_n^p and \hat{b}_n^p , with $k = 0 \dots \log_2(C) - 1$. The Bit Error Rate BER^p achieved by the spying antenna at position p is given by

$$BER^p = \frac{1}{N_{bits}} \sum_{j=0}^{N_{bits}-1} |\hat{d}_j^p - d_j|. \quad (6)$$

III. EXPERIMENTAL METHOD

The metric described in section II cannot be easily assessed experimentally since it requires the development of analog and digital communication modules at the transmitters and the receiver. Also, simultaneous transmission from M transmit antennas would require M frequency heads and amplifiers.

To perform experimental measurements of BER^p , we propose an experimental methodology with a low complexity, but that allows BER^p to be evaluated based on real over-the-air data transmission. This method is illustrated in Fig. 3.

Our experiment only relies on 1 generator with sampling frequency F_G , 1 oscilloscope with sampling frequency F_O , 1 amplifier with gain $\sqrt{\Gamma}$ and 1 computer. The latter is in charge of emulating both analog and digital signal processings and of monitoring the amplifier and the oscilloscope. The reciprocity of the channel is exploited: we assume than the forward links (from antennas i to antenna at position p) are identical to the reverse links (from antenna p to antennas i). Instead of using simultaneous transmission of multiple antennas, we process antennas successively, using a switch. Finally, instead of estimating the channel, computing the TR pre-filter and applying the pre-filter to the data, we first send the data through the wireless propagation channel, we store the received signal, and we transmit it in TR mode. TR is simply applied to both channel impulse response and data symbols, instead of channel alone.

Our method requires several successive steps and specific functions that are introduced hereafter. These phases (A,B,C,D,E,F and G) are detailed in Section IV.A,B,C,D,E, F and G, respectively.

In a first phase (A), the computer generates the data signal with sampling frequency F_G .

During a training phase (B), the generator sends the data signal over the air from the target antenna at position $p = 0$ to antenna i . This operation is repeated for every antenna i with the same data. Simultaneously, the oscilloscope acquires the signal received by antenna i . The computer then time inverses it, normalizes it, and finally stores it.

During a focusing phase (C), which is reiterated for every antenna i , and every position p of the spy antenna, the signal stored at antenna i by the computer during the training phase, is sent over the air by the generator towards the spy antenna at position p . Simultaneously, this focused signal from antenna i normally dedicated to receiver at position $p = 0$ but received at position p is stored by the computer.

During a combining phase (D), the computer combines, over antennas i , the focused signals determined during the

focusing phase for position p , and stores a unique focused signal for each position p .

Then, for each position p , the computer post-processes the focused signal obtained after the combining phase, and performs synchronization (E).

Finally, the demodulation, the Single Tap Receiver (F) and the spy BER computation (G) are performed by the computer, over sampled signals.

The BER^p metric measured using the methodology slightly differs from the one defined in section II. The receiver noise power is proportional to the number of antennas M . However, this introduces a fix bias in SNR for all positions p , which can easily be corrected by transmitting at M times higher power.

IV. DESCRIPTION OF THE DIFFERENT EXPERIMENT PHASES

A. Data Signal

The computer generates $d_{\log_2(C)n+i}$ and associated symbols $a_n + j b_n$ with $n = 0 \dots N_u - 1$, as described in section II. In addition, null symbols are added at the beginning and the end of the initial sequence:

$$a_n = b_n = 0 \quad \text{for} \quad -(N_1 - 1) \leq n < 0. \quad (7)$$

$$a_n = b_n = 0 \quad \text{for} \quad 0 \leq n - N_u < N_2. \quad (8)$$

Thus, contrary to previous section, indices $n \in S_{symbols} = [-(N_1 - 1), (N_u + N_2 - 1)]$. The corresponding interval, in time unit, in generator samples, and in oscilloscope samples are denoted S_{time} , S_G and S_O , respectively. $N_1 > 0$ is chosen so that most of the energy of the symbol $n = 0$ is captured, (i.e. $|f(t < -\frac{N_1}{B})| \ll |f(0)|$). As the generator and the oscilloscope are synchronized, they transmit and receive, respectively, during the same exact period. One must ensure that the oscilloscope entirely receives the signal sent by the generator, over-the-air even with propagation delay. Hence, $N_2 > 0$ is chosen so that $|h^{p,m}(t > \frac{N_2}{B})| \ll |h^{p,m}(t < \frac{N_2}{B})|$.

The computer emulates the following analog processing phases introduced in section II: filtering by $f(t)$, carrier modulation, $w^m(t)$ pre-filtering. Analog signals are replaced by signals sampled at F_G , and digital instead of analog processing is applied. The computer computes the data samples r_k , for $k \in S_G$, and the normalized sample s_k as follows:

$$r_k = \sum_{n \in S_{symbols}} \left(a_n \cos\left(\frac{k}{F_G}\right) + b_n \sin\left(\frac{k}{F_G}\right) \right) f\left(\frac{k}{F_G} - \frac{n}{B}\right), \quad (9)$$

$$s_k = \frac{r_k}{\max_{n \in S_G} (|r_l|)}. \quad (10)$$

B. Training of antenna i

This training procedure is described for a given antenna i . The generator transmits the following amplified analog signal $u(t)$ through the target antenna, with $t \in S_{time}$:

$$u(t) = \sqrt{F} \sum_{k \in S_G} s_k y(F_G t - k). \quad (11)$$

Simultaneously, the oscilloscope, switched over antenna i , receives the analog signal $v^{0,i}(t)$ after propagation through the wireless channel $h^{0,i}$, with $t \in S_{time}$:

$$v^{0,i}(t) = (h^{0,i} * u)(t). \quad (12)$$

The oscilloscope samples $z_k^{0,i}$ of $v^{0,i}(t)$, with $k \in S_O$, are:

$$z_k^{0,i} = v^{0,i}\left(\frac{k}{F_O}\right) + x_k^{0,i}, \quad (3)$$

where $x_k^{0,i}$ is the sampled thermal noise. The $z_k^{0,i}$ coefficients are sent to the computer, and converted into samples $y_k^{0,i}$ with sampling frequency F_G . For $k \in S_G$:

$$y_k^{0,i} = \frac{1}{2} (x_{k1}^{0,i} + x_{k1+1}^{0,i}), \quad (14)$$

with $k1 \in S_O$ such that:

$$\frac{k1}{F_O} \leq \frac{k}{F_G} < \frac{k1+1}{F_O}. \quad (15)$$

The computer performs time inversion and normalization:

$$S_k^{0,i} = \frac{y_{N_{\frac{F_O}{F_G}} - 1 - k}^{0,i}}{\max_{l \in S_G} (|y_l^{0,i}|)}. \quad (16)$$

C. Focusing phase for antenna i and position p

This training procedure is described for a given antenna i and a given position p . The generator and the amplifier send the following analog signal over the air, for $t \in S_{time}$:

$$U^{0,i}(t) = \sqrt{F} \sum_{k=1}^{N_G} S_k^{0,i} y(F_G t - k). \quad (17)$$

Simultaneously, the oscilloscope receives $V^{p,i}(t)$ at antenna i after propagation through wireless channel $h^{p,i}$, with $t \in S_{time}$:

$$V^{p,i}(t) = (h^{p,i} * U^{0,i})(t). \quad (18)$$

The oscilloscope samples $Z_k^{p,i}$ of $V^{p,i}(t)$, with $k \in S_O$, are:

$$Z_k^{p,i} = V^{p,i}\left(\frac{k}{F_O}\right) + X_k^{p,i}, \quad (19)$$

where $X_k^{p,i}$ is the sampled thermal noise. The computer converts the sampling frequency from F_O to F_G :

$$Y_k^{p,i} = \frac{1}{2} (X_{k1}^{p,i} + X_{k1+1}^{p,i}), \quad k \in S_G. \quad (20)$$

such that:

$$\frac{k1}{F_O} \leq \frac{k}{F_G} < \frac{k1+1}{F_O}. \quad (21)$$

D. Combined Focused signal for position p

The computer combines the $Y_k^{p,i}$ samples of focused signals of each antenna i . The resulting unique focused sampled signal γ_k^p , ($k \in S_G$) for position p , and its time inverse, ξ_k^p , are:

$$\gamma_k^p = \sum_{i=0}^{M-1} Y_k^{p,i}, \quad (22)$$

$$\xi_k^p = \gamma_{N_{\frac{F_G}{F_O}} - 1 - k}^p. \quad (23)$$

E. Emulating perfect synchronisation at the receiver

The focused signal ξ_k^p measured experimentally is delayed compared to the initial transmit signal s_k defined in (10), due to

propagation. This propagation delay is unknown, and has to be estimated experimentally by the computer. To study the confidentiality of the communication, we make sure that the achieved BER is not limited by the synchronization phase. To achieve ideal delay estimation, the entire sequence of reference symbols s_k is used to determine the propagation delay $k_{synchro}^p$ in generator samples (this method is of course not applicable in a real system):

$$k_{synchro}^p = \text{Arg}\{l, \max_l (\sum_{i=0}^{M-1} \xi_k^p s_{k+l})\}. \quad (24)$$

The synchronized signal, with $(k - k_{synchro}^p) \in S_G$ is:

$$\lambda_k^p = \xi_{k-k_{synchro}^p}^p. \quad (25)$$

F. Demodulation for position p , Single Tap Receiver

The computer emulates the analog demodulation by the following digital processing, with $(k - k_{synchro}^p) \in S_G$:

$$\omega_k^p = \lambda_k^p \cos\left(2\pi F_C \frac{k}{F_G}\right), \quad (26)$$

$$\vartheta_k^p = \lambda_k^p \sin\left(2\pi F_C \frac{k}{F_G}\right). \quad (27)$$

The computer emulates the analog filtering and the sampling (Single Tap Receiver). The symbols, with $n \in S_{symbols}$ are:

$$p_n^p = \sum_{(l-k_{synchro}^p) \in S_G} \omega_l^p f\left(\frac{l}{F_G} - \frac{n}{B}\right). \quad (28)$$

$$q_n^p = \sum_{(l-k_{synchro}^p) \in S_G} \vartheta_l^p f\left(\frac{l}{F_G} - \frac{n}{B}\right). \quad (29)$$

Then the computer extracts the useful symbols \hat{a}_n^p and \hat{b}_n^p :

$$\hat{a}_n^p = p_{N_1+n}^p \text{ for } 0 \leq n < N_u \quad (30)$$

$$\hat{b}_n^p = q_{N_1+n}^p \text{ for } 0 \leq n < N_u. \quad (31)$$

The required normalization of the received signal, before de-mapping to compensate for focusing and propagation, is unknown. The normalization has to be estimated experimentally. As for synchronization, in order to achieve ideal normalization estimation, we use the entire sequence as a reference. The optimum normalization ζ^p is found as follows:

$$\zeta^p = \text{Arg}\left\{c, \min_{\zeta} \left(\sum_{n=0}^{N-1} (\zeta \hat{a}_n^p - a_n)^2 + (\zeta \hat{b}_n^p - b_n)^2 \right) \right\}. \quad (32)$$

The estimated symbols are then normalized before being de-mapped, for $0 \leq n < N_u$, the computer updates \hat{a}_n^p and \hat{b}_n^p :

$$\hat{a}_n^p = \zeta^p \hat{a}_n^p. \quad (33)$$

$$\hat{b}_n^p = \zeta^p \hat{b}_n^p. \quad (34)$$

G. BER evaluation for position p

The same method as for the system described in II is used to evaluate BER^p .

V. MEASUREMENTS RESULTS AND ANALYSIS

BER^p has been assessed using the experimental methodology described in section III, with a measurement setup illustrated in the Fig. 2. The following parameters were used: $B = 30$ MHz, $F_C = 1$ GHz (this corresponds to a

wavelength of 30 cm), $F_G = 4.2$ GHz, $F_O = 5$ GHz, $\beta = 0.22$. The constellation was size $C = 256$, 256QAM mapping and de-mapping was implemented in the computer. The BER^p measurements have been performed in a room with $M = 16$ distributed antennas, and along 4 axis (P1, P2, P3 and P4). BER^p is plotted in Fig.4 as a function of the spy-to-target distance. The spy-to-target receive power ratio is plotted in Fig. 5. While the spy BER and power measurements are precise (low error on y-axis), the measurements of the positions of antennas is “noisy”. Indeed, antennas were moved manually using un-precise carriages. We estimate that there is a +2/-2cm error on the distances reported on these figures (x-axis). This explains the “not smooth” aspect of the curves.

Nevertheless, even with these measurement impairments, even in conditions which are not favorable to focusing (with a bandwidth as low as 30MHz, and even with a large amount of antennas being in Line Of Sight conditions), the measurements, strongly show a BER “sink” and a power “bell”, and confirm the confidentiality advantages given by TR technique, in addition to green aspects.

Moreover, we can note there that we also assumed that the required time for carrying all the operations was smaller than the coherence time of the channel. The results obtained with the experiment confirm the validity of this assumption, in a room where useless movements were avoided during the experiment. In the framework of the French ANR TRIMARAN project, a MISO TR platform will be developed that will allow further results to be obtained under other indoor propagation conditions. Such experiments are important to demonstrate the spatial focusing of TR and specifically the BER at a non target antenna position due to the difficulty in obtaining them by simulation tools.

VI. CONCLUSION

We have characterized the confidentiality of a time reversal communication system in indoor, through an experimental measurement of the BER achieved by a spy antenna nearby the target antenna. The measurements clearly show a spy BER “sink” centered on the target. MISO TR can therefore be used as a secrete communication mean in an indoor communication owing to its high focusing gains but also to the very poor performance attained by a spy antenna as soon as it is not placed at the target antenna place. This experiment is of importance because if simulations tools can easily help to demonstrate focusing gains in the time domain, they do not simply allow the evaluation of the spatial behavior and their BER associated performance around the target antenna.

ACKNOWLEDGMENT

This work has been sponsored by Agence Nationale de la Recherche (ANR) project TRIMARAN and supported by “Pôle de compétitivité Images et réseaux”. The authors would like to thank Mr. Youmni Ziade and Mr. Hacene Azzouz for their contributions to this work.

REFERENCES

- [1] A. Derode, P. Roux, and M. Fink, "Robust Acoustic Time Reversal With High Order Multiple Scattering," *Phys. Rev. Letters*, vol. 75, pp. 4206-4209, 1995.
- [2] A. Derode, A. Tourin, J. de Rosny, M. Tanter, S. Yon, and M. Fink. Taking advantage of multiple scattering to communicate with time reversal antennas. *Phys. Rev. Lett.*, 90 :014301, 2003.
- [3] A. Paulraj, R. Nabar, D. Gore, "Introduction to Space-Time Wireless Communications", Cambridge Univeristy Press, 2003.
- [4] C. Oestges, J. Hansen, S. M. Emami, A. D. Kim, G. Papanicolaou, and A. J. Paulraj, "Time Reversal Techniques for Broadband Wireless Communication Systems," European Microwave Conference (Workshop), Amsterdam, The Netherlands, pp. 49-66 , Oct 2004.
- [5] B. Wang; Y. Wu; F. Han; Y.-H. Yang; Liu, K.J.R.; , "Green Wireless Communications: A Time-Reversal Paradigm," *Selected Areas in Communications, IEEE Journal on* , vol.29, no.8, pp.1698-1710, September 2011.
- [6] I. Hoydis; M. Kobayashi; M. Debbah; "Green Small-Cell Networks" *Vehicular Technology Magazine, IEEE*, vol.6, no.1, pp.37-43, March 2011.
- [7] H. T. Nguyen, J. B. Andersen, and G. F. Pedersen, "The Potential Use of Time Reversal Techniques in Multiple Element Antenna Systems", *Communication Letters, IEEE*, vol 9, no. 1, january, 2005.
- [8] R. C. Qiu, C. Zhou, N. Guo, and J. Q. Zhang, "Time Reversal With MISO for Ultrawideband Communications: Experimental Results", *Antennas and wireless propagation letters, IEEE*, vol. 5, 2006.
- [9] A. Khaleghi, G. El Zein, I. H. Naqvi, "Demonstration of Time-Reversal in Indoor Ultra-Wideband Communication: Time Domain Measurement", *IEEE ISWCS*, 2007.
- [10] N. Guo, B. M. Sadler, and R. C. Qiu "Reduced-Complexity UWB Time-Reversal Techniques and Experimental Results", *Transactions on wireless communications, IEEE*, vol. 6, no. 12, december 2007
- [11] C. Zhou, N. Guo, and R. C. Qiu, "Time-Reversed Ultra-wideband (UWB) Multiple Input Multiple Output (MIMO) Based on Measured Spatial Channels", *Transactions on vehicular technology, IEEE*, vol. 58, no. 6, july 2009.
- [12] Y. Song, N. Guo, Z. Hu, and R. C. Qiu, "FPGA Based UWB MISO Time-Reversal System Design and Implementation", *Proceedings of 2010 IEEE International Conference on Ultra-Wideband (ICUWB2010)*
- [13] H. El-Sallabi, P. Kyritsi, A. Paulraj, and G. Papanicolaou "Experimental Investigation on Time Reversal Precoding for Space-Time Focusing in Wireless Communications", *Transactions on instrumentation and measurement, IEEE*, vol. 59, no. 6, june 2010
- [14] G. Geraci, J. Yuan, A. Razi and I. B. Colling, "Secrecy Sum-Rates for Multi-User MIMO Linear Precoding", *8th International Symposium on Wireless Communication Systems*, Aachen, 2011
- [15] ANR Trimaran project. VERSO 2010 program. <http://www.agence-nationale-recherche.fr/projet-anr/>

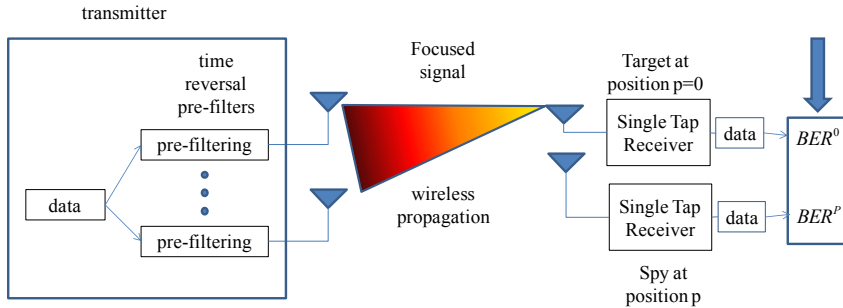


Fig. 1. Spy BER evaluation.

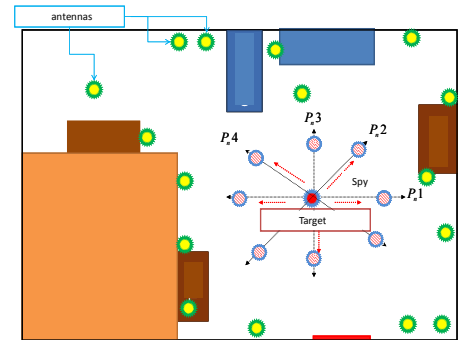


Fig. 2. Room and positions of antennas.

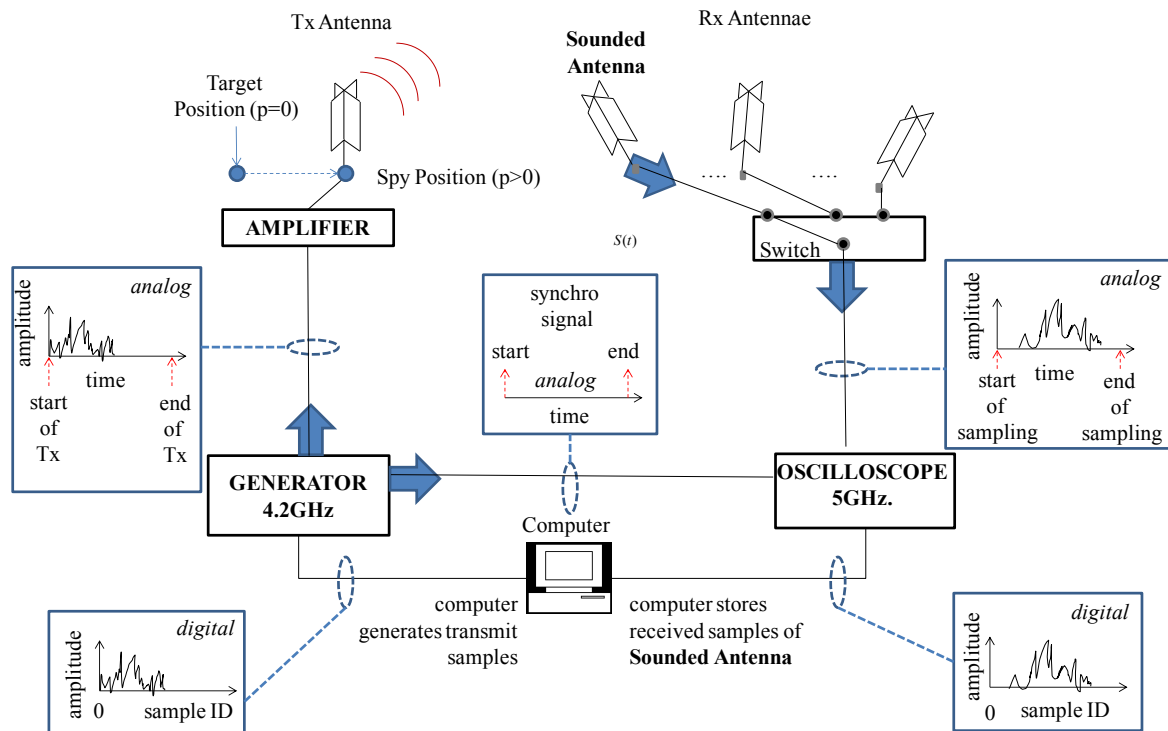


Fig. 3. Experimental Setup: focusing phase, for spy position p and antenna i .

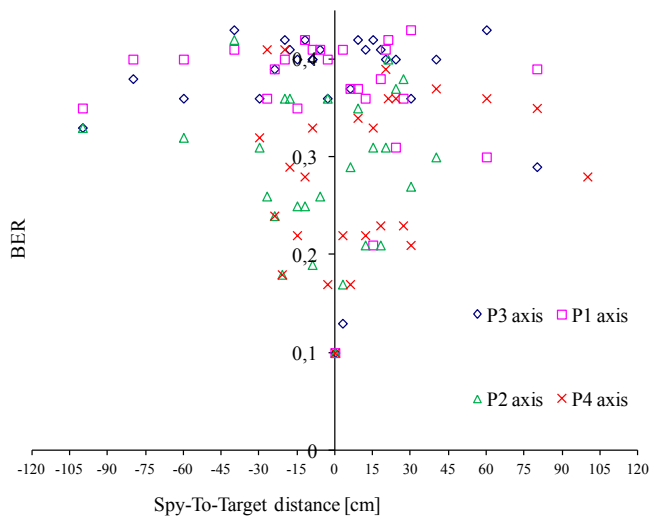


Fig. 4. Spy BER

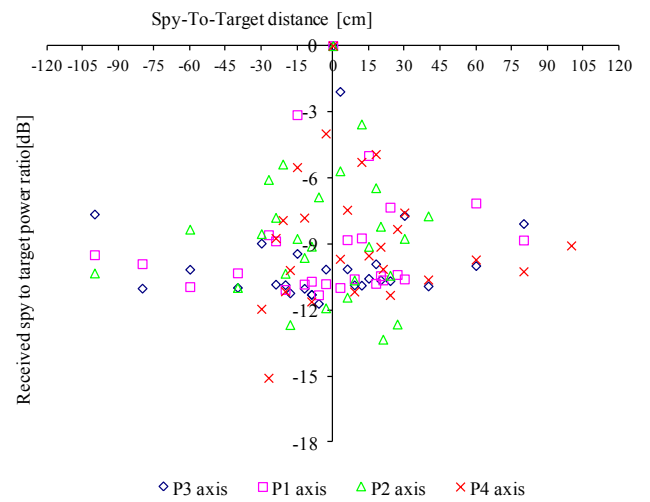


Fig. 5. Spy to target received power ratio[dB]